Rational Design of Highly Selective Spleen Tyrosine Kinase Inhibitors

Matthew C. Lucas,*[†,§] David M. Goldstein,[†,∥] Johannes C. Hermann,[†] Andreas Kuglstatter,[†] Wenjian Liu,[‡] Kin Chun Luk,[†] Fernando Padilla,[†] Michelle Slade,[†] Armando G. Villaseñor,[†] Jutta Wanner,[†] Wenwei Xie,[‡] Xiaohu Zhang,[‡,⊥] and Cheng Liao[†]

[†]Small Molecule Research, Discovery Chemistry, pRED, Pharma Research and Early Development, Hoffmann-La Roche Inc., 340 Kingsland Street, Nutley, New Jersey 07110, United States

[‡]BioDuro(Beijing)Co., Ltd., Building E, No. 29, Life Science Park Road, Changping District, Beijing 102206, P. R. China

S *Supporting Information*

ABSTRACT: A novel approach to design selective spleen tyrosine kinase (Syk) inhibitors is described. Inhibition of spleen tyrosine kinase has attracted much attention as a mechanism for the treatment of autoimmune diseases such as asthma, rheumatoid arthritis, and SLE. Fostamatinib, a Syk inhibitor that successfully completed phase II clinical trials, also exhibits some undesirable side effects. More selective Syk inhibitors could offer safer, alternative treatments. Through a systematic evaluation of the kinome, we identified Pro455 and Asn457 in the Syk ATP binding site as a rare combination among sequence aligned kinases and hypothesized that optimizing the interaction between them and a Syk inhibitor molecule would impart high selectivity for Syk over other kinases. We report the structure-guided identification of three series of selective spleen tyrosine kinase inhibitors that support our hypothesis and offer useful guidance to other researchers in the field.
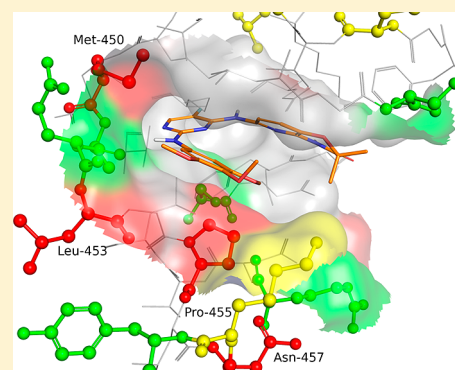
INTRODUCTION

Spleen tyrosine kinase (Syk) is an intracellular protein tyrosine kinase whose signaling pathway is largely involved in the adaptive immune response but also in some innate and nonimmune functions.[1] Syk is most widely expressed in hematopoietic cells but is also expressed in other tissues. It serves as a key mediator of B-cell receptor- and Fc receptor-mediated signaling in inflammatory cells such as B cells, mast cells, macrophages, dendritic cells, and neutrophils and is involved in bone resorption by osteoclasts.[2−4] Upon receptor stimulation, Syk becomes activated primarily by SRC family tyrosine kinase Lyn and subsequently transduces the signal through VAV family members, phospholipase Cγ (PLCγ), the regulatory subunits of phosphoinositide 3-kinases (PI3Ks) and SH2 domain containing leukocyte proteins (SLP) SLP76 and SLP65. The resulting activation of various downstream components leads to cellular responses including cytokine release, differentiation, proliferation, reactive oxygen species (ROS) production, cytoskeletal rearrangement, and survival. No human patients with a spontaneous mutation in Syk have been described, although recently there was a description of a family carrying a 5.3 Mb microdeletion. The deletion involves 30 genes, including the immunologically active SYK gene.[5] Fostamatinib **1**, a poorly selective Syk inhibitor, recently completed phase II trials for the treatment of rheumatoid arthritis (Figure 1).[6] In these studies adverse effects included hypertension, gastrointestinal effects (nausea and diarrhea), and neutropenia. In addition, a Syk selective siRNA (Excellair) successfully completed phase I trials and advanced into a phase II clinical trial in asthma in September 2009 (inhaled administration).[7] No adverse effects were noted in the phase I trial. PRT062607, reported to be a Syk specific inhibitor,[7] is currently in phase II, but no data related to adverse events have been described.

The SYK gene has also been disrupted in mice. The absence of the viable kinase results in perinatal lethality (due to a defect in lymphatic vascular development) and a lack of mature B cells.[8] Syk^{−/−} reconstituted mice are unable to promote B-cell maturation because of failure of the ProB to PreB transition.[9] These mice are protected from autoantibody-induced arthritis in a K/BxN model.[10] Collectively these data support a role for Syk in B-cell signaling and rheumatoid arthritis. Indeed, Syk inhibitors are efficacious in rodent arthritis models and have been shown to suppress arthritis scores, bone erosions, pannus formation, and synovitis. Syk inhibitors have also shown efficacy in in vivo animal models of asthma, idiopathic thrombocytopenic purpura, systemic lupus erythematous, and autoimmune diabetes. In human cell lines, Syk inhibitors are able to inhibit BCR-mediated B-cell activation, FcεR-mediated mast cell and basophil responses, and Fcγ-mediated mono-cytes/macrophage response and block osteoclast differentiation; these cell types are implicated in the onset and propagation of autoimmune disease and the cartilage and bone destruction associated with rheumatoid arthritis.[11−20]
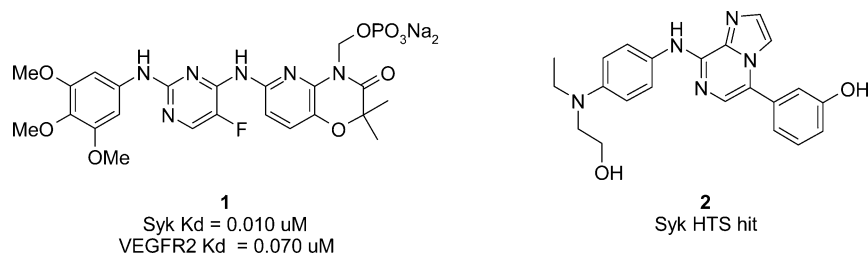
Figure 1. Structure of fostamatinib **1** and Syk high-throughput screening hit **2**.

Collectively, the clinical trial data and the critical role of B cells in human autoimmune and inflammatory diseases make Syk a compelling drug target in the therapeutic areas of rheumatoid arthritis, SLE, B-cell malignancies, asthma, and allergic upper airway disorders.[21−23]

While there has been significant effort to find Syk inhibitors in recent years, few of these have advanced into clinical trials. The limited or unknown selectivity over the human kinome of those molecules that have made it as far as the clinic makes interpretation of the clinical benefit of Syk inhibition challenging and ambiguous. The most advanced of these, **1**, has a poor selectivity profile, and it is likely that some of the reported safety concerns and even some of the efficacy observed are a consequence of off-target kinase activity. For example, **1** is a potent inhibitor of the kinase VEGFR2; it is widely reported that such inhibitors cause elevated blood pressure.[24] It is also a strong inhibitor of the kinase c-RET. This particular kinase is critical for renal and ureteric development, and its inhibition may have resulted in the developmental toxicity of **1** observed in rabbits.[25]

As a result, we were compelled to develop rational approaches to generate highly selective Syk inhibitors that could help to improve and advance our understanding of the relevance of Syk in disease and enable the determination of the potential of a selective Syk inhibitor to replicate the clinical benefits displayed by fostamatinib while minimizing the off-target effects that may limit or prevent its use in a clinical setting. Our ultimate vision was to create a safer, efficacious drug candidate for the treatment of autoimmune diseases. Recently, Portola Pharmaceuticals reported detailed results of selective Syk inhibitors, and the presented biochemical, cellular, and animal data support our aim to identify highly selective Syk inhibitors to maximize clinical benefit.[7] We have confirmed some of the Portola data to allow us to benchmark our own efforts in this regard (Table 1). Herein we present an approach that enabled the rational design of selective Syk inhibitors and disclose selective in vitro tools.

■ SYNTHESIS

The syntheses of the compounds described are shown (Schemes 1−6; see Supporting Information). The thiazolopyrimidines were all synthesized from the commercially available dichlorothiazolopyrimidine **15**. This was converted to **16** via a regioselective nucleophilic aromatic substitution of the C7-chlorine. Suzuki coupling gave ester **17**, which could be easily converted to **3** in three steps via saponification, amide coupling, and a final saponification (Scheme 1). Compounds **6−9** were synthesized from **16** through a Buchwald−Hartwig amination followed by deprotection, amide bond formation, and a final deprotection to give the final compounds (Schemes 2 and 3). The triazolopyridine **4** was synthesized via a Suzuki and Buchwald−Hartwig coupling sequence (Scheme 4). In the case

Table 1

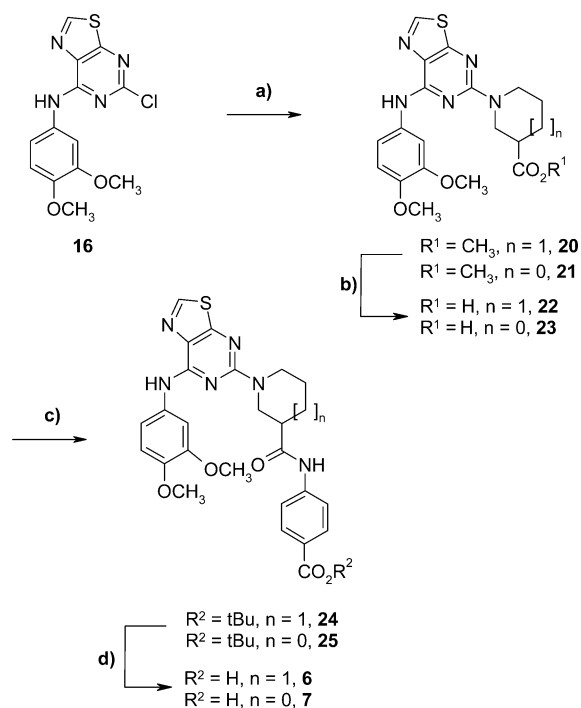| compd	Syk IC$_{50}$ (nM)^a	LE^b	Ramos B cell IC$_{50}$ (μM)^c	LYSA solubility (μg/mL)^d	selectivity (no. of kinases inhibited >90% at 10 μM)^e
PRT062607	1	0.41	0.223	<1	116/385
1^f	17	0.31	0.267	<1	145/290
3	7	0.29	0.156	<1	14/386
4	3	0.31	0.444	<1	34/386
5	1	0.32	0.482	<1	

^{a}See Supporting Information for details. Data shown are the average of at least n = 2. ^{b}Ligand efficiency (in energy units/atom ≈ (kcal/mol)/atom). ^{c}See Supporting Information for details. ^{d}Lyophilized solubility assay data. ^{e}DiscoveRx KINOMEscan screening platform measurements employing an active site-directed competition binding assay to quantitatively measure interactions between test compounds and 290−386 kinase assays. ^{f}Data shown are for the active entity R406, (fostamatinib is a prodrug).

Scheme 1. Synthesis of Thienopyrimidine 3^a

R^2 = CH$_3$, **17**
c) R^2 = H, **18**

R^3 = tBu, **19**
e) R^3 = H, **3**
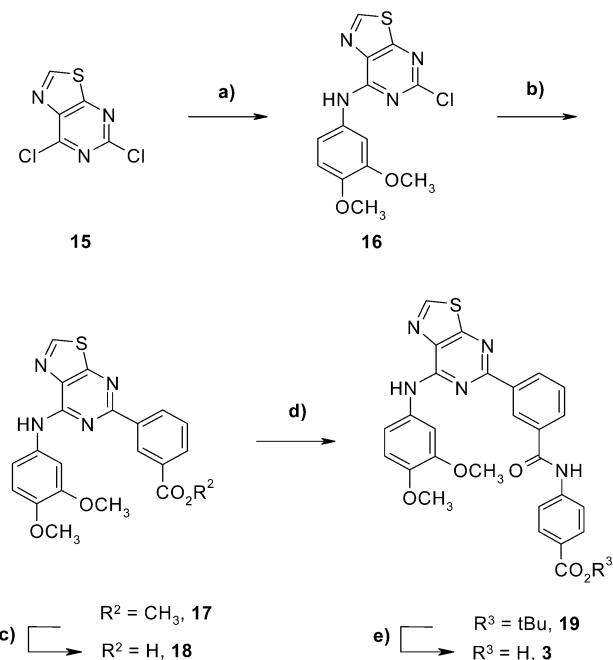
^{a}Reagents and conditions: (a) 3,4-dimethoxyaniline, DIPEA, DMSO, rt, 2 h, 64%; (b) 3-(4,4,5,5-tetramethyl[1,3,2]dioxaborolan-2-yl)-benzoic acid methyl ester, 1,4-dioxane, H$_2$O, Na$_2$CO$_3$, Pd(PPh$_3$)$_4$, 100 °C, 16 h, 81%; (c) NaOH, THF, H$_2$O, rt, 16 h, 98%; (d) *tert*-butyl 4-aminobenzoate, EDCI, DMAP, DMF, rt, 2 h, 70%; (e) CF$_3$CO$_2$H, CH$_2$Cl$_2$, rt, 15 h, 66%.

of imidazopyridazines **5** and **10−14**, the 2-aminopyridine was installed first, via a regioselective nucleophilic aromatic
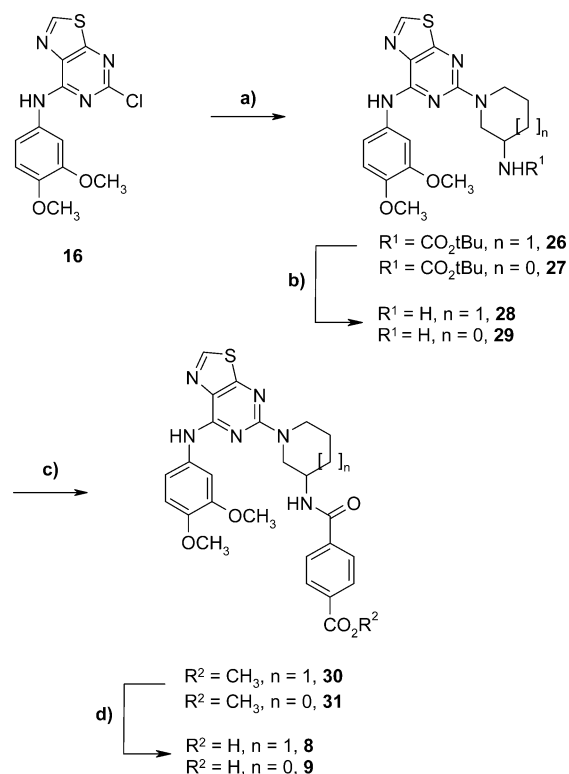
Scheme 2. Synthesis of Thienopyrimidines 6 and 7[a]

R[1] = CH$_3$, n = 1, **20**
R[1] = CH$_3$, n = 0, **21**

R[1] = H, n = 1, **22**
R[1] = H, n = 0, **23**

R[2] = tBu, n = 1, **24**
R[2] = tBu, n = 0, **25**

R[2] = H, n = 1, **6**
R[2] = H, n = 0, **7**

[a]Reagents and conditions: (a) n = 1, methylpiperidine 3-carboxylate, Cs$_2$CO$_3$, X-Phos, Pd$_2$(dba)$_3$, 110 °C, 15 h, 56%; n = 0, methylpyrrolidine 3-carboxylate, Cs$_2$CO$_3$, X-Phos, Pd$_2$(dba)$_3$, 95 °C, 24 h, 89%; (b) NaOH, THF, MeOH, rt, 24 h, 98% (n = 1); NaOH, MeOH, rt, 24 h, 61% (n = 0); (c) HATU, DIPEA, DMF, rt, 72 h, 92% (n = 1), 77% (n = 0); (d) CF$_3$CO$_2$H, CH$_2$Cl$_2$, rt, 24 h, 37% (n = 1), 59% (n = 0).

Scheme 3. Synthesis of Thienopyrimidines 8 and 9[a]

R[1] = CO$_2$tBu, n = 1, **26**
R[1] = CO$_2$tBu, n = 0, **27**

R[1] = H, n = 1, **28**
R[1] = H, n = 0, **29**

R[2] = CH$_3$, n = 1, **30**
R[2] = CH$_3$, n = 0, **31**

R[2] = H, n = 1, **8**
R[2] = H, n = 0, **9**

[a]Reagents and conditions: (a) n = 1, tert-butyl piperidin-3-yl-carbamate, X-Phos, Cs$_2$CO$_3$, dioxane, Pd$_2$(dba)$_3$, 95 °C, 24 h, 93%; n = 0, tert-butyl pyrrolidin-3-yl carbamate, X-Phos, Cs$_2$CO$_3$, dioxane, Pd$_2$(dba)$_3$, 95 °C, 24 h, 88%; (b) HCl, dioxane, rt, 24 h, 100%; (c) 4-methoxybenzoic acid, HATU, DIPEA, DMF, rt, 2 h, then EDCI, DMAP, 4 days, 96% (n = 1), 88% (n = 0); (d) LiOH, H$_2$O, MeOH, THF, 2 h, rt, 18% (n = 1), 47% (n = 0).

displacement of the bromine, and this was followed by the aryl–aryl bond creation through a Suzuki coupling (Schemes 5 and 6).

■ RESULTS AND DISCUSSION

We began our endeavor by analyzing the Syk ATP binding site structure and comparing it with other aligned kinase structures to identify commonality with respect to amino acid residue incidences (Figure 2). Four amino acid residues were identified that rarely appeared in other kinase active sites: Met450, Leu453, Pro455, and Asn457 (each having an incidence in less than 5% of all kinases, Figure 2b). On the basis of our examination of the binding pocket, we felt that Pro455 and Asn457 were the most attractive as targets for optimization of the interaction between them and putative ATP-competitive spleen tyrosine kinase inhibitors. The spatial proximity of Pro455 and Asn457 suggested we might be able to design inhibitors that interacted with these two simultaneously. On the other hand, Leu453, with its side chain projecting out and away from the ATP-binding site did not offer as many opportunities for targeting. Met450, while proximal, offered a smaller accessible surface area with which to interact, so we chose not to focus on this residue in our initial exploration.

Pro455 is present in only 9 aligned kinases (of a total of 433), while Asn457 is present in 21 aligned kinases. Pro455, a hydrophobic residue, is most commonly replaced with hydrophilic or charged residues, while Asn457, an acidic residue, is most commonly replaced by hydrophobic residues. Thus, we predicted that a small molecule that either had

favorable hydrophobic interactions with Pro455 or formed attractive electrostatic interactions with Asn457 would result in selective Syk inhibition. Furthermore, simultaneously achieving favorable interactions with Pro455 *and* Asn457 (an incidence that is present in only one other kinase, MLK1) seemed to have the potential to afford exquisite selectivity over the kinome. We were encouraged by the observation that the X-ray crystal structure of the active component of nonselective Syk kinase inhibitor **1** showed a suboptimal interaction with Pro455 and no discernible interaction with Asn457 or Met450 (Figure 2a).[26]

Following a high throughput screening campaign, we had identified the imidazopyrazine scaffold (e.g., **2**, Figure 1) and selected this as a starting point for our investigation. Imidazopyrazines as kinase hinge binders were familiar to us from our own, and others', effort to develop kinase inhibitors.[27,28] While Btk inhibitors containing the imidazopyrazine hinge binding motif have been reported to bind to the kinase active site in an extended "N"-conformation,[28] this conformation seemed awkward and unsatisfactory when applied to the Syk ATP binding pocket. An X-ray crystal structure obtained of **2** bound to the Syk kinase domain (Figure 3) suggested to us that vectors from the 6-position of the imidazopyrazine might offer the ability to project toward the Asn457 residue via a bent, "inverted U-conformation". The aniline projecting out of the front of the binding site already appeared to make some hydrophobic interactions with the

Scheme 4. Synthesis of Triazolopyridine 4[a]
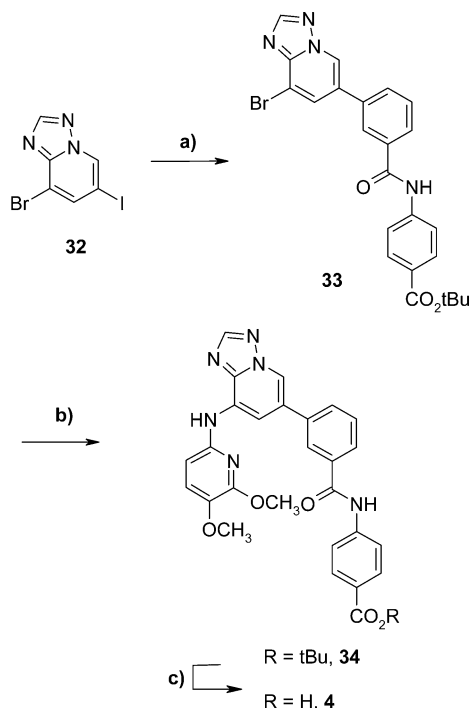
[a]Reagents and conditions: (a) *tert*-butyl 4-(3-(4,4,5,5-tetramethyl-1,3,2-dioxaborolan-2-yl)benzamido)benzoate, Na$_2$CO$_3$, H$_2$O, dioxane, Pd(PPh$_3$)$_4$, 96 °C, 24 h, 44%; (b) 5,6-dimethoxypyridin-2-amine, X-Phos, Cs$_2$CO$_3$, dioxane, Pd$_2$(dba)$_3$, 95 °C, 24 h, 44%; (c) CF$_3$CO$_2$H, CH$_2$Cl$_2$, rt, 24 h, 59%.

Scheme 5. Synthesis of Imidazopyridazine 5[a]
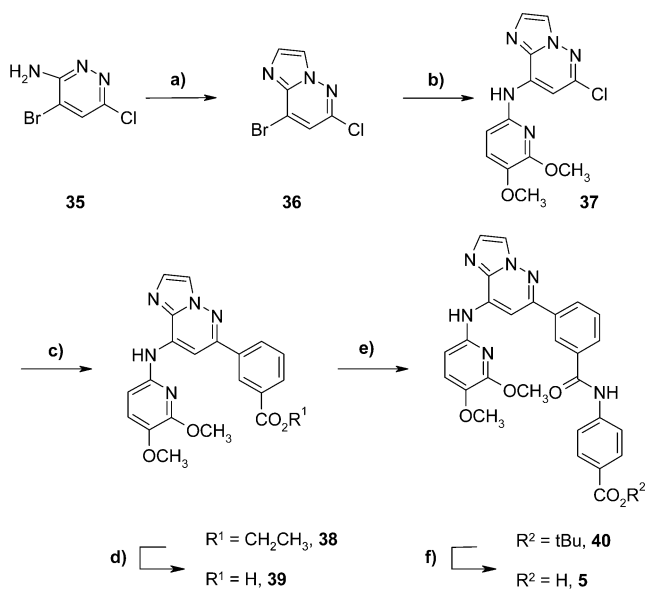
[a]Reagents and conditions: (a) 2-chloro-1,1-diethoxyethane, PTSA, *i*-PrOH, 80 °C, 20 h, 98%; (b) 5,6-dimethoxypyridin-2-amine, DMF, NaH, rt, 15 h, 91%; (c) ethyl 3-(4,4,5,5-tetramethyl-1,3,2-dioxaborolan-2-yl)benzoate, K$_3$PO$_4$, X-Phos, dioxane, water, Pd$_2$(dba)$_3$, 125 °C, MW, 60 min, 34%; (d) LiOH, dioxane, H$_2$O, rt, 4 h, 88%; (e) *tert*-butyl 4-aminobenzoate, 1-methyl-1*H*-imidazole, EDCI, DMF, 16 h, rt, 55%; (f) CF$_3$CO$_2$H, CH$_2$Cl$_2$, rt, 24 h, 39%.

Pro455 and was expected to provide a good basis for optimization.

Scheme 6. Synthesis of Imidazopyridazines 10−14[a]
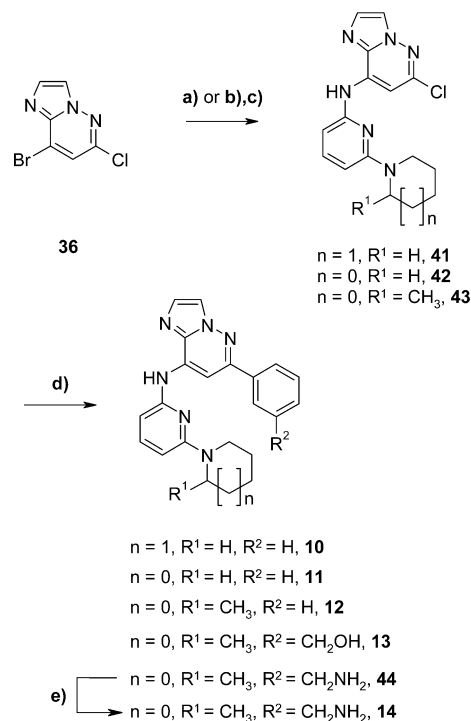
[a]Reagents and conditions: (a) *n* = 1, R^1 = H, 6-(piperidin-1-yl)pyridin-2-amine, NaH, DMF, rt, 16 h, 24%; (b) 6-fluoropyridin-2-amine, NaH, DMF, rt, 16 h, 99%; (c) pyrrolidine, H$_2$O, 205 °C, microwave, 30 min, 18% (*n* = 0, R^1 = H); 2-methylpyrrolidine, H$_2$O, 205 °C, microwave, 30 min, 64% (*n* = 0, R^1 = CH$_3$); (d) PhB(OH)$_2$, Pd$_2$(dba)$_3$, X-Phos, K$_2$CO$_3$, dioxane, water, 100 °C, 4 h, 58% (*n* = 1, R^1 = H, R^2 = H); PhB(OH)$_2$, Pd$_2$(dba)$_3$, X-Phos, K$_2$CO$_3$, dioxane, water, 100 °C, 4 h, 78% (*n* = 0, R^1 = H, R^2 = H); PhB(OH)$_2$, Pd$_2$(dba)$_3$, X-Phos, K$_2$CO$_3$, dioxane, water, 100 °C, 4 h, 40% (*n* = 0, R^1 = CH$_3$, R^2 = H); R^2-PhB(OH)$_2$, X-Phos, K$_2$CO$_3$, dioxane, H$_2$O, Pd$_2$(dba)$_3$, 100 °C, 3 h, 81% (*n* = 0, R^1 = H, R^2 = CH$_2$OH); R^2-PhB(OH)$_2$, X-Phos, Na$_2$CO$_3$, dioxane, H$_2$O, Pd$_2$(dba)$_3$, 95 °C, 15 h, 52% (*n* = 0, R^1 = H, R^2 = CN); (e) LiAlH$_4$, THF, 2 h, rt, 53%.

Thus, we initiated an effort to support our selectivity hypothesis and to deliver selective tool molecules to enable internal biological investigation and validation of Syk as a worthy target for pharmacological intervention.

The crowded chemical space surrounding the imidazopyrazine screening hit **2** led us to investigate alternative hinge binding cores from which we could expand our hit to lead activities. Multiple heterocyclic alternatives were explored based on their ability to mimic the same hinge binding interactions. Ultimately, we focused on the thiazolopyrimidines, triazolopyridines, and imidazopyridazines described herein (Figure 4). The thiazolopyrimidines had the advantage that chemical manipulation was more facile and that when A is phenyl, very few literature or patent examples were uncovered. The triazolopyridine Markush structure was novel, and to the best of our knowledge, this remains an under-represented kinase binding motif in the literature. Finally, the imidazopyridazine Markush structure also appeared only sparsely in the patent literature at that time, and we had in-house experience with it. The majority of our SAR work focused on the thiazolopyrimidines that could be easily substituted in the 6-position, which in our view offered the best vector to reach and interact with both the Pro455 and the Asn457 residues (vide infra).
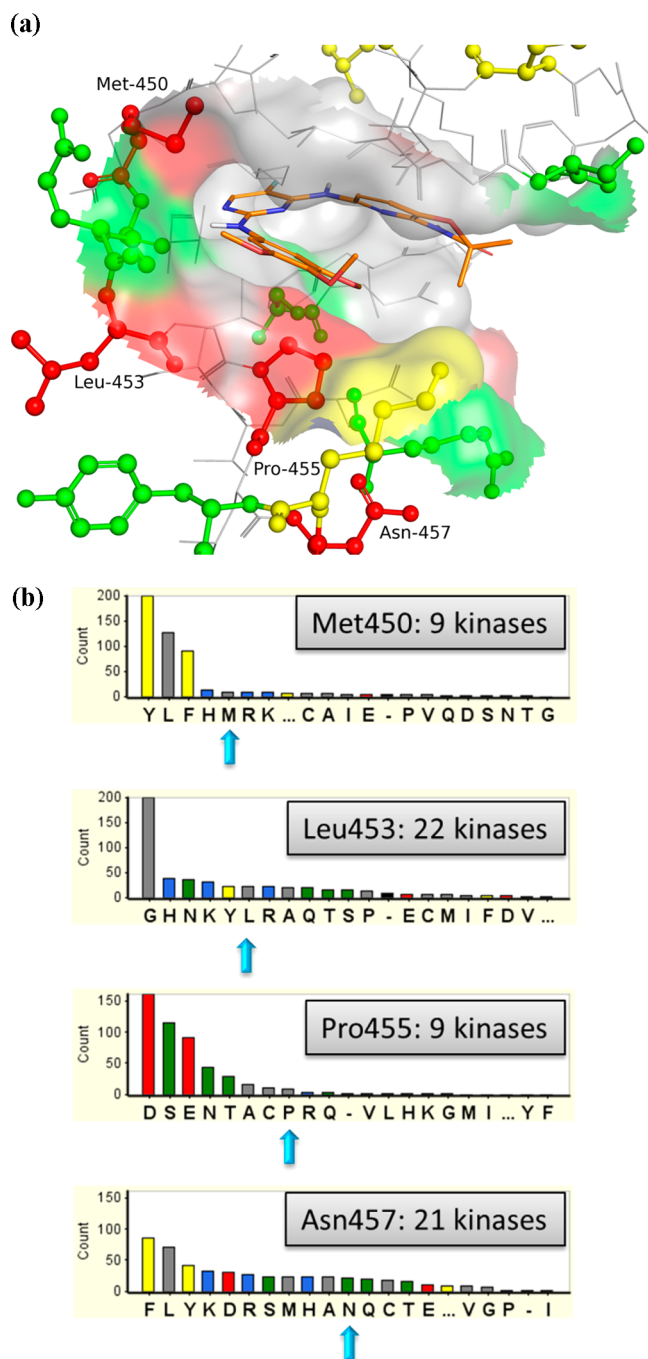
(a)

(b)

Figure 2. (a) Schematic of Syk ATP-binding site illustrating incidence of individual residues in a total of 433 aligned kinases. Incidence key is as follows: red, 1−21; yellow, 22−46; green, 50−92; blue, 93−433. The figure is based on the crystal structure of Syk in complex with **1** (PDB accession number 3FQS, **1** is colored orange and shown as sticks).[26] The residues with lowest incidence, Met450, Leu453, Pro455, and Asn457 are labeled. (b) Incidence of Met450, Leu453, Pro455, and Asn457 residues in a total of 433 aligned kinases and comparison to other residues. Yellow bars indicate aromatic residues. Gray bars indicate hydrophobic residues. Blue indicates basic residues. Red indicates acidic residues, and green represents polar residues.

The evolution of our Hit to lead effort is summarized in Figure 5. As mentioned above, we had extensive experience working with imidazopyrazine containing Btk inhibitor scaffolds, and we expected that similar scaffolds, where cycle A was a phenyl group, would offer opportunities to explore
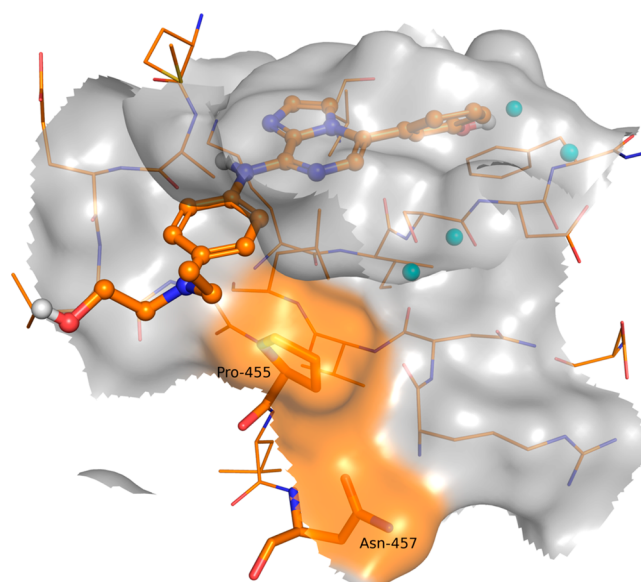

Figure 3. X-ray crystal structure of high throughput screening hit, imidazopyrazine **2**, bound to Syk (2.3 Å resolution, PDB accession number 4FYN). The scaffold provides the appropriate vectors from the core heterocycle to project toward the Pro455 and Asn457 residues (highlighted in orange).
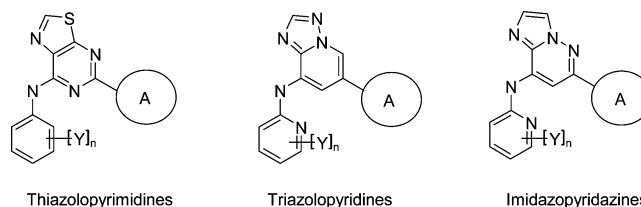

Figure 4. Markush structures of thiazolopyrimidines, triazolopyridines, and imidazopyridazines, substituted in the 6-position with generic cyclic group A.

ways of extending downward and adjacent to the Pro455, as well as reaching the Asn457. Indeed, hit expansion around our initial HTS hit had shown that several related compounds, where A was phenyl, showed submicromolar Syk inhibition. We chose to carry out our initial exploration using dimethoxyphenylaniline or 5,6-dimethoxy-2-aminopyridine functionality at the left-hand side of the molecule (i.e., Y = OMe, $n = 2$, Figure 4). The reason for this was twofold: First, the methoxy functional group is fairly innocuous and was unlikely to interfere with late stage chemical transformations, and second, our own past experience as well as extensive Syk literature (including R406) had taught us that this group would likely offer good intrinsic Syk potency. We expected that later, once potent, selective Syk inhibitors had been identified, we would be able to manipulate these solvent exposed groups to modify the biopharmaceutical properties of the scaffold, if needed.

On the basis of our continuous monitoring and analysis of emerging imidazopyrazine and Syk literature, we identified a number of potential R^1 groups that might be of the correct topology to interact with the Pro455 and the Asn457 amino acid side chains.[29] Ultimately, benzoylaminobenzoic acid containing groups were identified that provided highly potent inhibitors of Syk (**3**−**5**, Figure 6). When tested in our Ramos B-cell assay, we were encouraged that these compounds exhibited potencies commensurate with that of **1**. Yet when the kinome selectivity of **3** and **4** against a panel of 386 kinases was assessed
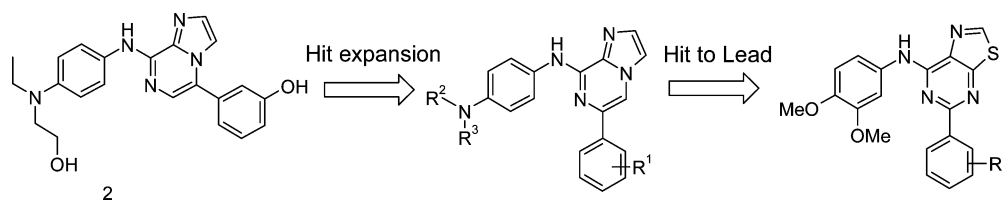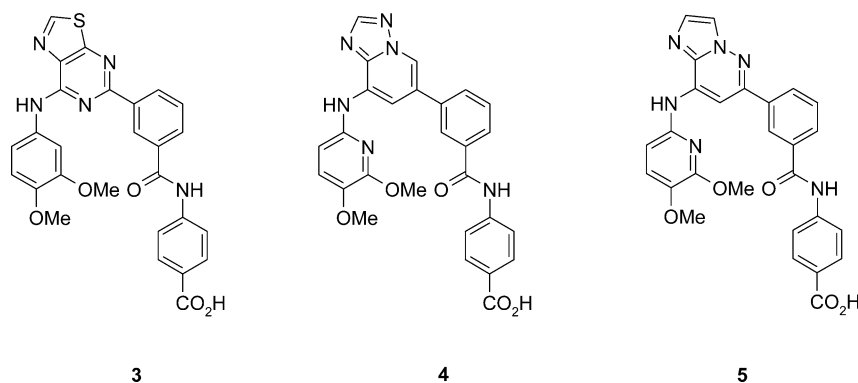
Figure 5. Evolution of Hit to lead.

Figure 6. Representative, potent examples of new Syk inhibitors.

(DiscoveRx ScanMax), it was found to be far superior to **1**, suggesting that the desired interaction between Pro455 and Asn457 could be giving rise to enhanced selectivity (Figure 7, panels a, b, c, e). We obtained an X-ray crystal structure that confirmed the interactions (unpublished results). Encouraged, we began to focus on assessing the biopharmaceutical properties of the compounds. In general, the compounds were stable in liver microsomes; however, the permeability of

Figure 7. DiscoveRx kinase screening dendrograms at 10 μM compound. The KINOMEscan screening platform employs an active site-directed competition binding assay to quantitatively measure interactions between test compounds and 386 kinase assays. Images were generated using TREE*spot* software tool and reprinted with permission from KINOMEscan, a division of DiscoveRx Corporation, Copyright DISCOVERX CORPORATION 2010: (a) fostamatinib parent R406; (b) thiazolopyrimidine **3**; (c) triazolopyridine **4**; (d) imidazopyridazine **13**; (e) legend showing circle size and its correlation to the percent inhibition described for inhibition of kinases represented in dendrograms.

these carboxylic acids was poor (data not shown). The kinetic solubility for **3**–**5** was also poor, all showing LYSA solubility of <1 (Table 1).

Since the ratio of sp^3 to sp^2 centers in a molecule is predictive of druglikeness and developability,[30] we addressed this in our new Syk inhibitor scaffolds by replacing some of the sp^2 centers, anticipating that this would also improve the solubility. Modeling highlighted the potential of pyrrolidines and piperidines to replace the central phenyl while retaining a conformation that could maintain simultaneous interactions with Pro455 and Asn457. The preferred replacement was not obvious from modeling, as we were unsure of the requirement for any hydrogen bonding interactions between the linker amide and the binding pocket. The thiazolopyrimidine series was selected for further exploration because of its synthetic tractability. Deterioration of potency occurred with all four modifications, and yet **6** and **9** kept respectable potency (Table 2). The kinase selectivity was measured and was excellent. An X-ray crystal structure of **9** bound to Syk was obtained and confirmed that hydrophobic interactions between the two phenyl groups of **9** with Pro455 and a polar interaction between the carboxylic acid and Asn457 were occurring (Figure 8). This provided excellent support for our selectivity hypothesis. We were pleased to find that in most cases (e.g., **7**–**9**, Table 2) our measured solubility also significantly improved. However, the improved solubility did not translate into improved cellular potency, suggesting that permeability, not solubility, was the prevalent driver of the cellular readout. Thus, we considered ways of improving the intrinsic permeability of the molecules and focused in particular on replacing the carboxylic acid functional group.

Unfortunately, our SAR studies demonstrated that deleting the carboxylate moiety led to significant loss of binding potency. Without the critical ionic interaction to act as an "anchor" it is likely that other binding conformations occur and that the close interaction with Pro455 and the distal phenyl is also lost. Simple alternative functional groups to replace the carboxylic acid (e.g., a methylamide), as well as more complex
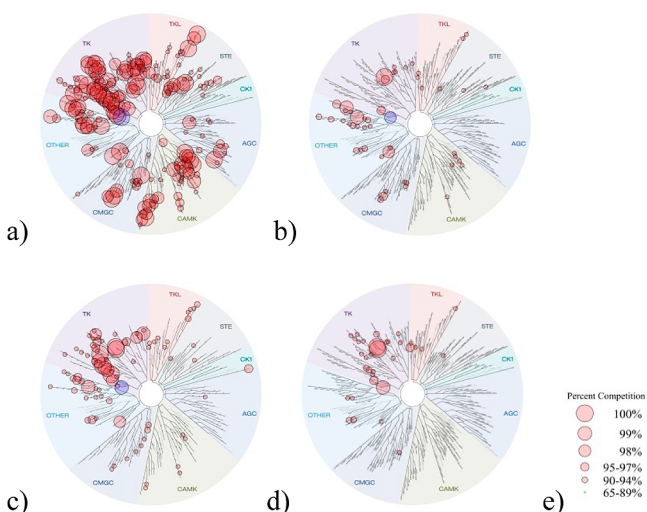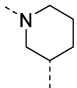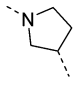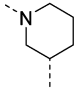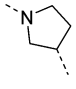
Table 2. Inhibition of Syk Activity by Thiazolopyrimidines and Kinase Selectivity

Compound	Ring	Syk IC$_{50}$ (nM)[a]	LE[b]	Ramos B cell IC$_{50}$ (μM)[c]	LYSA solubility (μg/mL)[d]	Selectivity (no. of kinases inhibited >90% at 10 μM)[e]
6	piperidine	50	0.26	0.741	<1	13/386
7	pyrrolidine	93	0.26	5.60	94	-
8	piperidine	423	0.23	7.80	32	-
9	pyrrolidine	47	0.27	6.27	204	12/386

[a]See Supporting Information for details. Data shown are the average of at least $n = 2$. [b]Ligand efficiency (in energy units/atom ≈ (kcal/mol)/atom). [c]See Supporting Information for details. [d]Lyophilized solubility assay data. [e]DiscoveRx KINOMEscan screening platform measurements employing an active site-directed competition binding assay to quantitatively measure interactions between test compounds and 386 kinase assays.
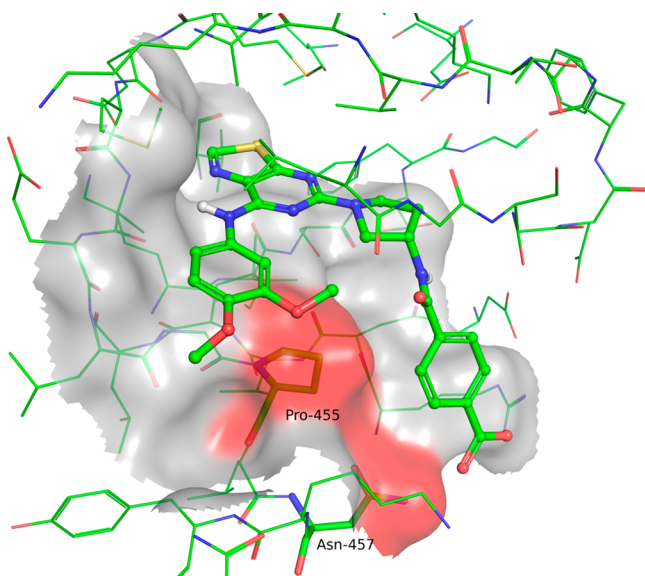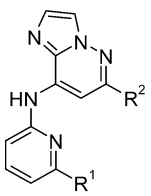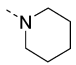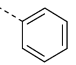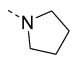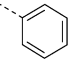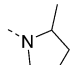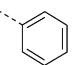

Figure 8. X-ray cocrystal structure of thiazolopyrimidine **9** (depicted in green) bound to Syk (1.4 Å resolution, PDB accession number 4FYO). The Pro455 and Asn457 are highlighted in red.

heterocyclic bioisosteres of carboxylic acids that covered a calculated pK_a range of 4−9 (e.g., 4-methyl-4H-[1,2,4]triazole-3-thiol, [1,3,4]oxadiazole-2-thiol, 1,2,4-oxadiazol-5-one), were investigated but generally led to some deterioration in potency (data not shown). The doggedly low ligand efficiency, high molecular weight, and restricted opportunities to replace the carboxylic acid prompted us to investigate whether disregarding the Asn457 and focusing instead on optimizing interactions with only the Pro455 residue could still provide Syk selective compounds. Reducing the molecular weight and addressing the poor permeability that seemed to accompany the ca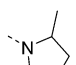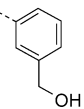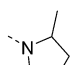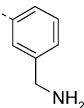rboxylate moiety were also expected to improve the biopharmaceutical properties of the scaffolds. We also chose to return to structures containing a phenyl linker, despite the high sp^2 ratio, since these had provided our most cell potent examples. Pro455 was most readily accessed from vectors extending from the left-hand side 2-aminopyridine or aniline moiety. We excluded the thiazolopyrimidine core from this exercise, as it did not offer the ability to lock the conformation of the aniline ring and may have led to ambiguous data as we sought to project groups over the proline ring. In contrast, the triazolopyridine and imidazopyridazine series, each possessing 2-aminopyridine front groups, were conformationally rigid and thus more suitable. We ultimately selected the imidazopyridazine core for

Table 3. Inhibition of Syk Activity by Imidazopyridazine Analogues 10−14

10 - 14

Compound	R^1	R^2	Syk IC$_{50}$ (nM)[a]	LE[b]	Ramos B cell IC$_{50}$ (μM)[c]	LYSA solubility (μg/mL)[d]	Selectivity (no. of kinases inhibited >90% at 10 μM)[e]
10			406	0.31	-	<1	-
11			351	0.33	-	<1	-
12			127	0.34	-	<1	-
13			25	0.35	0.359	<1	11/386
14			16	0.35	0.581	<1	-

[a]See Supporting Information for details. Data shown are the average of at least n = 2. [b]Ligand efficiency (in energy units/atom ≈ (kcal/mol)/atom). [c]See Supporting Information for details. [d]Lyophilized solubility assay data. [e]DiscoveRx KINOMEscan screening platform measurements employing an active site-directed competition binding assay to quantitatively measure interactions between test compounds and 386 kinase assays.

this investigation, since it represented the most ligand efficient starting point.

We prioritized pyridine substituents that appeared to interact well with Pro455 during computational modeling. Among these, pyridines substituted in the 6-position with N-linked pyrrolidine and piperidine emerged as particularly promising groups to target the proline aliphatic ring (Table 3, 10−12). Substituents on the pyrrolidine ring were chosen for their potential to "surround" the proline residue and further optimize van der Waals interactions. The crystal structure of 12 bound to the Syk protein was solved and indicated a close contact between the 2-methylpyrrolidine and the Pro455 side chain (Figure 9). However, enzyme potency of 10−12 was suboptimal, and despite the significant reduction in molecular weight, measured solubility remained poor, likely because of the high clogP for these compounds.

Follow-up compounds were prioritized that were expected to reduce the clogP of the molecules and thus improve their biopharmaceutical properties. We hoped that in addition to improving physicochemical properties, the polar functionality might introduce additional opportunities to form polar interactions and result in improved potency, thus enabling a better comparison of kinome selectivity profiles. Among the compounds investigated, substitution on the phenyl linker provided some of our most promising compounds. For example, benzyl alcohol 13 and benzylamine 14 retained good ligand efficiencies (Table 3). Benzyl alcohol 13 was highly selective (Figure 7d and Table 3). The X-ray structure was solved for benzylamine 14 and confirmed that the proline remained in van der Waals contact with the pyrrolidine ring (not shown). This provided excellent evidence that optimization of hydrophobic interactions with the Pro455 alone is sufficient to achieve highly selective Syk inhibition. All crystal structures solved with a methylpyrrolidine showed a single enantiomer bound, with the chiral methyl group pushing up and interacting with the glycine loop. This was somewhat unexpected, and we cannot rule out that this could also be contributing to the good selectivity profile. Indeed, inhibitors of other kinases such as Pfizer's Jak3 inhibitor tofacitinib gain selectivity by making a Gly loop interaction, albeit in this case through hydrophilic substructure interactions rather than the hydrophobic interaction reported here.[31] Thus, we were able to
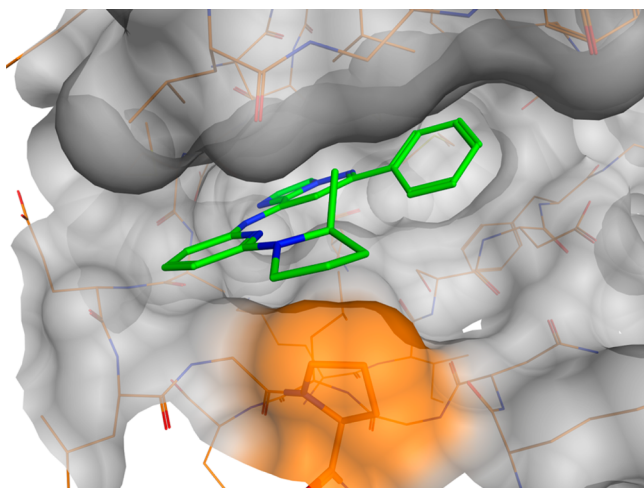
Figure 9. Crystal structure of **12** bound to Syk (1.85 Å resolution, PDB accession number 4FZ6). The hydrophobic interaction between the pyrrolidine ring and Pro455 (surface shaded orange) is apparent. Note that only a single enantiomer was observed in the crystal structure.

identify molecules that allowed us to drastically reduce the molecular weight and obtain cell potent Syk selective inhibitors. However, despite respectable cell potency, we were unable to achieve suitable combinations of permeability and solubility, and ultimately the pharmacokinetics of these compounds did not allow full in vivo characterization.

CONCLUSION

We report the rational design of selective Syk inhibitors by analyzing the kinase binding pocket to identify residues with low incidence among other kinases. This provides essential proof of concept for this design strategy which can be applied to all kinase targets. We have described three scaffolds that are able to interact with Asn457 and/or Pro455 to achieve excellent Syk selectivity in vitro. Unfortunately, the physicochemical challenges with these scaffolds proved to be intractable and prevented us from carrying out in vivo studies to assess the effect of Syk selective inhibition in animal models of autoimmunity and cancer. However, the hypothesis described has enabled us to design multiple new scaffolds with improved ligand efficiencies and physicochemical properties. The application of our strategy to generate and optimize other, structurally differentiated, selective Syk inhibitor scaffolds with good pharmacokinetic properties for the treatment of autoimmune diseases will be the subject of future communications.

ASSOCIATED CONTENT

ⓢ Supporting Information

Full experimental details and characterization of synthetic intermediates and final products; experimental procedure for the Syk biochemical and cell based assay. This material is available free of charge via the Internet at http://pubs.acs.org.

AUTHOR INFORMATION

Corresponding Author

*Phone: (408) 585-8051. E-mail: matthew.lucas@cubist.com.

Present Addresses

§Cubist Pharmaceuticals, 65 Hayden Avenue, Lexington, MA 02421, U.S.

‖Principia BioPharma, Inc., 400 E. Jamie Court, No. 302, South San Francisco, CA 94080, U.S.

⊥School of Pharmaceutical Sciences, Soochow University, 199 Ren Ai Road, Suzhou, Jiangsu, P. R. China.

ABBREVIATIONS USED

BCR, B-cell receptor; Btk, Bruton's tyrosine kinase; DIPEA, diisopropylethylamine; EDCI, 1-ethyl-3-(3-dimethylaminopropyl)carbodiimide; HATU, (2-(7-aza-1H-benzotriazole-1-yl)-1,1,3,3-tetramethyluronium hexafluorophosphate; Jak, Janus kinase; MeOH, methanol; MLK1, mixed-lineage kinase 1; MW, microwave; $Pd_2(dba)_3$, tris-(dibenzylideneacetone) dipalladium(0); PLCγ, phospholipase Cγ; PTSA, p-toluenesulfonic acid; RET, rearranged during transfection tyrosine kinase; siRNA, small inhibitory ribonucleic acid; SLE, systemic lupus erythematous; SLP, SH2 domain containing leukocyte protein; Syk, spleen tyrosine kinase; VEGFR2, vascular endothelial growth factor receptor 2; X-Phos, 2-dicyclohexylphosphino-2′,4′,6′-triisopropylbiphenyl

REFERENCES

(1) Mocsai, A.; Ruland, J.; Tybulewicz, V. L. J. The SYK tyrosine kinase: a crucial player in diverse biological functions. *Nat. Rev. Immun.* **2010**, *10*, 387−402.

(2) Bajpai, M.; Chopra, P.; Dastidar, S. G.; Ray, A. Spleen tyrosine kinase: a novel target for therapeutic intervention of rheumatoid arthritis. *Expert Opin. Invest. Drugs* **2008**, *17*, 641−659.

(3) Zou, W.; Kitaura, H.; Reeve, J.; Long, F.; Tybulewicz, V. L.; Shattil, S. J.; Ginsberg, M. H.; Ross, F. P.; Teitelbaum, S. L. Syk, c-Src, the alphavbeta3 integrin, and ITAM immunoreceptors, in concert, regulate osteoclastic bone resorption. *J. Cell Biol.* **2007**, *176*, 877−888.

(4) Koga, T.; Inui, M.; Inoue, K.; Kim, S.; Suematsu, A.; Kobayashi, E.; Iwata, T.; Ohnishi, H.; Matozaki, T.; Kodama, T.; Taniguchi, T.; Takayanagi, H.; Takai, T. Costimulatory signals mediated by the ITAM motif cooperate with RANKL for bone homeostasis. *Nature* **2004**, *428*, 758−763.

(5) Siggberg, L.; Peippo, M.; Sipponen, M.; Miikkulainen, T.; Shimojima, K.; Yamamoto, T.; Ignatius, J.; Knuutila, S. 9q22 deletion-first familial case. *Orphanet J. Rare Dis.* **2011**, *6*, 45.

(6) Tam, F. W. K.; McAdoo, S. P. Fostamatinib disodium. *Drugs Future* **2011**, *36*, 273−280.

(7) (a) ZaBeCor News. Press Release September 14, 2009. http://www.zabecor.com/news/. (b) Coffey, G.; DeGuzman, F.; Inagaki, M.; Pak, Y.; Delaney, S. M.; Ives, D.; Betz, A.; Jia, Z. J.; Pandey, A.; Baker, D.; Hollenbach, S. J.; Phillips, D. R.; Sinha, U. Specific inhibition of spleen tyrosine kinase suppresses leukocyte immune function and inflammation in animal models of rheumatoid arthritis. *J. Pharmacol. Exp. Ther.* **2012**, *340*, 350−359.

(8) Turner, M.; Mee, P. J.; Costello, P. S.; Williams, O.; Price, A. A.; Duddy, L. P.; Furlong, M. T.; Geahlen, R. L.; Tybulewicz, V. L. J. Perinatal lethality and blocked B-cell development in mice lacking the tyrosine kinase Syk. *Nature* **1995**, *378*, 298−302.

(9) Cheng, A. M.; Rowley, B.; Pao, W.; Hayday, A.; Bolen, J. B.; Pawson, T. Syk tyrosine kinase required for mouse viability and B-cell development. *Nature* **1995**, *378*, 303−306.

(10) Jakus, Z.; Simon, E.; Balázs, B.; Mócsai, A. Genetic deficiency of Syk protects mice from autoantibody-induced arthritis. *Arthritis Rheum.* **2010**, *62*, 1899−1910.

(11) Pine, P. R.; Chang, B.; Schoettler, N.; Banquerigo, M. L.; Wang, S.; Lau, A.; Zhao, F.; Grossbard, E. B.; Payan, D. G.; Brahn, E.

Inflammation and bone erosion are suppressed in models of rheumatoid arthritis following treatment with a novel Syk inhibitor. *Clin. Immunol.* **2007**, *124*, 244−257.

(12) Braselmann, S.; Taylor, V.; Zhao, H.; Wang, S.; Sylvain, C.; Baluom, M.; Qu, K.; Herlaar, E.; Lau, A.; Young, C.; Wong, B.; Lovell, S.; Sun, T.; Park, G.; Argade, A.; Jurcevic, S.; Pine, P.; Singh, R.; Grossbard, E. B.; Payan, D. G.; Masuda, E. S. R406, an orally available spleen tyrosine kinase inhibitor blocks Fc receptor signaling and reduces immune complex-mediated inflammation. *J. Pharmacol. Exp. Ther.* **2006**, *319*, 998−1008.

(13) Krishnan, S.; Juang, Y. T.; Chowdhury, B.; Magilavy, A.; Fisher, C. U.; Nguyen, H.; Nambiar, M. P.; Kyttaris, V.; Weinstein, A.; Bahjat, R.; Pine, P.; Rus, V.; Tsokos, G. C. Differential expression and molecular associations of Syk in systemic lupus erythematosus T cells. *J. Immunol.* **2008**, *181*, 8145−8152.

(14) Nathan, A. T.; Peterson, E. A.; Chakir, J.; Wills-Karp, M. Innate immune responses of airway epithelium to house dust mite are mediated through beta-glucan-dependent pathways. *J. Allergy Clin. Immunol.* **2009**, *123*, 612−618.

(15) Wills-Karp, M.; Nathan, A.; Page, K.; Karp, C. L. New insights into innate immune mechanisms underlying allergenicity. *Mucosal Immunol.* **2010**, *3*, 104−110.

(16) LeibundGut-Landmann, S.; Grob, O.; Robinson, M. J.; Osorio, F.; Slack, E. C.; Tsoni, S. V.; Schweighoffer, E.; Tybulewicz, V.; Brown, G. D.; Ruland, J.; Reis e Sousa, C. Syk- and CARD9-dependent coupling of innate immunity to the induction of T helper cells that produce interleukin 17. *Nat. Immunol.* **2007**, *8*, 630−638.

(17) Gringhuis, S. I.; Dunnen, J. E.; Litjens, M.; van der Vlist, M.; Wevers, B.; Bruijns, S. C.; Geijtenbeek, T. B. Dectin-1 directs T helper cell differentiation by controlling noncanonical NF-kappaB activation through Raf-1 and Syk. *Nat. Immunol.* **2009**, *10*, 203−213.

(18) Saijo, S.; Ikeda, S.; Yamabe, K.; Kakuta, S.; Ishigame, H.; Akitsu, A.; Fujikado, N.; Kusaka, T.; Kubo, S.; Chung, S. H.; Komatsu, R.; Miura, N.; Adachi, Y.; Ohno, N.; Shibuya, K.; Yamamoto, N.; Kawakami, K.; Yamasaki, S.; Saito, T.; Akira, S.; Iwakura, Y. Dectin-2 recognition of alpha-mannans and induction of Th17 cell differentiation is essential for host defense against *Candida albicans*. *Immunity* **2010**, *32*, 681−691.

(19) Robinson, M. J.; Osorio, F.; Rosas, M.; Freitas, R. P.; Schweighoffer, E.; Gross, O.; Verbeek, J. S.; Ruland, J.; Tybulewicz, V.; Brown, G. D.; Moita, L. F.; Taylor, P. R.; Reis e Sousa, C. Dectin-2 is a Syk-coupled pattern recognition receptor crucial for Th17 responses to fungal infection. *J. Exp. Med.* **2009**, *206*, 2037−2051.

(20) Zarbock, A.; Lowell, C. A.; Ley, K. Spleen tyrosine kinase Syk is necessary for E-selectin-induced alpha(L)beta(2) integrin-mediated rolling on intercellular adhesion molecule-1. *Immunity* **2007**, *26*, 773−783.

(21) Weinblatt, M. E.; Kavanaugh, A.; Burgos-Vargas, R.; Dikranian, A. H.; Medrano-Ramirez, G.; Morales-Torres, J. L.; Murphy, F. T.; Musser, T. K.; Straniero, N.; Vicente-Gonzales, A. V.; Grossbard, E. Treatment of rheumatoid arthritis with a Syk kinase inhibitor: a twelve-week, randomized, placebo-controlled trial. *Arthritis Rheum.* **2008**, *58*, 3309−3318.

(22) Friedberg, J. W.; Sharman, J.; Sweetenham, J.; Johnston, P. B.; Vose, J. M.; LaCasce, A.; Schaefer-Cutillo, J.; De Vos, S.; Sinha, R.; Leonard, J. P.; Cripe, L. D.; Gregory, S. A.; Sterba, M. P.; Lowe, A. M.; Levy, R.; Shipp, M. A. Inhibition of Syk with fostamatinib disodium has significant clinical activity in non-Hodgkin lymphoma and chronic lymphocytic leukemia. *Blood* **2010**, *115*, 2578−2585.

(23) Meltzer, E. O.; Berkowitz, R. B.; Grossbard, E. B. An intranasal Syk-kinase inhibitor (R112) improves the symptoms of seasonal allergic rhinitis in a park environment. *J. Allergy Clin. Immunol.* **2005**, *115*, 791−796.

(24) Granger, J. P. Vascular endothelial growth factor inhibitors and hypertension: a central role for the kidney and endothelial factors? *Hypertension* **2009**, *54*, 465−467.

(25) Clemens, G. R.; Schroeder, R. E.; Magness, S. H.; Weaver, E. V.; Lech, J. W.; Taylor, V. C.; Masuda, E. S.; Baluom, M.; Grossbard, E. B. Developmental toxicity associated with receptor tyrosine kinase Ret inhibition in reproductive toxicity testing. *Birth Defects Res., Part A* **2009**, *85*, 130−136.

(26) Villaseñor, A. G.; Kondru, R.; Ho, H.; Wang, S.; Papp, E.; Shaw, D.; Barnett, J. W.; Browner, M. F.; Kuglstatter, A. Structural insights for design of potent spleen tyrosine kinase inhibitors from crystallographic analysis of three inhibitor complexes. *Chem. Biol. Drug Des.* **2009**, *73*, 466−470.

(27) Kondru, R. K.; Lou, Y.; Sjogren, E. B.; Soth, M. PCT Int. Appl. WO2010006970A1, 2010.

(28) Di Paolo, J. A.; Huang, T.; Balazs, M.; Barbosa, J.; Barck, K. H.; Bravo, B. J.; Carano, R. A.; Darrow, J.; Davies, D. R.; DeForge, L. E.; Diehl, L.; Ferrando, R.; Gallion, S. L.; Giannetti, A. M.; Gribling, P.; Hurez, V.; Hymowitz, S. G.; Jones, R.; Kropf, J. E.; Lee, W. P.; Maciejewski, P. M.; Mitchell, S. A.; Rong, H.; Staker, B. L.; Whitney, J. A.; Yeh, S.; Young, W. B.; Yu, C.; Zhang, J.; Reif, K.; Currie, K. S. Specific Btk inhibition suppresses B cell- and myeloid cell-mediated arthritis. *Nat. Chem. Biol.* **2011**, *7*, 41−50.

(29) Mitchell, S. A.; Currie, K. S.; Blomgren, P. A.; Armistead, D. M.; Raker, J. PCT Int. Appl. WO20090102468, 2009.

(30) Lovering, F.; Bikker, J.; Humblet, C. Escape from flatland: increasing saturation as an approach to improving clinical success. *J. Med. Chem.* **2009**, *52*, 6752−6756.

(31) Chrencik, J. E.; Patny, A.; Leung, I. K.; Korniski, B.; Emmons, T. L.; Hall, T.; Weinberg, R. A.; Gormley, J. A.; Williams, J. M.; Day, J. E.; Hirsch, J. L.; Kiefer, J. R.; Leone, J. W.; Fischer, H. D.; Sommers, C. D.; Huang, H. C.; Jacobsen, E. J.; Tenbrink, R. E.; Tomasselli, A. G.; Benson, T. E. Structural and thermodynamic characterization of the TYK2 and JAK3 kinase domains in complex with CP-690550 and CMP-6. *J. Mol. Biol.* **2010**, *400*, 413−433.